

Silica-supported Z-selective Ru olefin metathesis catalysts

Marc Renom-Carrasco^a, Philipp Mania^a, Reine Sayah^a, Laurent Veyre^a, Giovanni Occhipinti^b, Vidar R. Jensen^b, Chloé Thieuleux^{a,*}

^a Université de Lyon, Institut de Chimie de Lyon, C2P2 UMR 5265 CNRS-Université Lyon 1-CPE Lyon, ESCPE Lyon, 43, Bd du 11 Novembre 1918, 69616 Villeurbanne, France

^b Department of Chemistry, University of Bergen, Allégaten 41, N-5007 Bergen, Norway

ARTICLE INFO

Keywords:

Olefin metathesis
Z-selectivity
Ruthenium
NHC
Supported complexes

ABSTRACT

Recently reported thiolate-coordinated ruthenium alkylidene complexes show promise in Z-selective and stereoretentive olefin metathesis reactions. Herein we describe the immobilization of three Ru complexes containing a bulky aryl thiolate on mesostructured silica via surface organometallic chemistry. The applied methodology gives isolated catalytic sites homogeneously distributed on the silica surface. The catalytic results with two model substrates show comparable Z-selectivities to those of the homogeneous counterparts.

1. Introduction

Olefin metathesis is a well-known and established reaction for the formation of C=C bonds [1]. Since its discovery, many generations of catalysts, with improved activities and stabilities, have been developed. However, the olefin metathesis product is a thermodynamic mixture of the two alkene stereoisomers (Z and E), with the E-isomer normally being the favored one. In 2009, the first highly Z-selective olefin metathesis catalysts, based on Mo and W, were reported by Schrock and Hoveyda [2]. Improved versions of these catalysts [3] and also a highly E-stereoretentive catalyst [4] were later reported. The evolution of Z-selective and stereoretentive Ru-olefin metathesis catalysts has followed a similar chronology, starting by the reports of Grubbs and co-workers in 2011 [5]. Since then, two kinds of Z-selective Ru olefin metathesis catalysts and one highly stereoretentive have been reported (Fig. 1): cyclometalated N-heterocyclic carbene (NHC) architectures [6] and 2,4,6-arylbenzenethiolate-Ru complexes [7], and catecholthiolate-Ru complexes [8].

The immobilization of complexes onto solid supports is a recurrent strategy to avoid some of the problems associated with homogeneous catalysis [9]. Numerous groups have reported the immobilization of Ru olefin metathesis catalysts on different supports [10]. Here, we have chosen mesostructured silica supports, since they provide high surface areas, a good chemical stability and big pores avoiding mass transfer limitation during the catalytic reaction. They can be functionalized with homogeneously distributed organic tethers/ligands, which intermolecular distance can be controlled. This key asset allows to generate

isolated sites for the immobilization of organometallic complexes. This feature, in combination with the rigidity of the surface (not present in polymers for example), avoids any possible interaction between the metallic centers and allows the selective coordination of the complex on a single surface site. As any other heterogeneous support, it also allows an easy recovery of the metal (no pollution of the reaction products) and a good reusability if the active centers are still alive after catalysis. In this context, our group has already reported the usefulness of this kind of supports by immobilizing Ru olefin metathesis complexes on surface NHC ligands and, besides high catalytic performances, we also showed the presence of additional interactions between the silica surface and the metal when flexible tethers are used [11]. These specific interactions were found to provide an extra stabilization of the supported complexes. More recently, we also demonstrated that the anchoring of Ru-alkylidene complexes could also be successful by an anionic exchange of the chloride by a propyl or phenyl thiolate (Fig. 2) [12].

The success of this latter methodology prompted us to investigate the immobilization of different Ru-alkylidene complexes through a sterically demanding aryl thiolate, mimicking the molecular structure of the Jensen-Occhipinti complexes (Fig. 1), in order to obtain, for the first time, an immobilized Z-selective Ru olefin metathesis catalyst. The results presented below demonstrate that the supported catalyst can perform as well as the molecular analogue.

* Corresponding author.

E-mail address: thieuleux@cpe.fr (C. Thieuleux).

<https://doi.org/10.1016/j.mcat.2019.110743>

Received 30 September 2019; Received in revised form 18 November 2019; Accepted 12 December 2019

2468-8231/ © 2019 Elsevier B.V. All rights reserved.

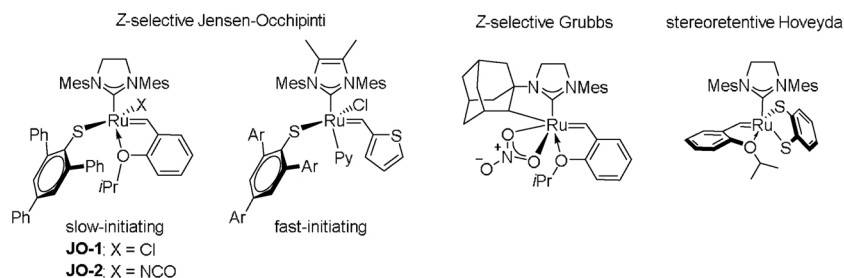


Fig. 1. Reported Z-selective and stereoretentive Ru olefin metathesis catalysts.

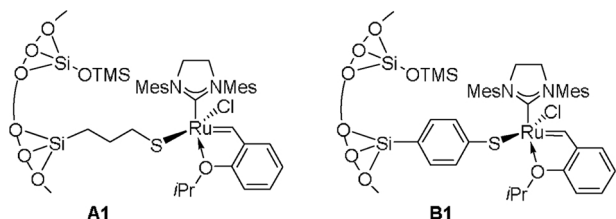


Fig. 2. Reported Ru olefin metathesis catalysts supported on SiO₂ via a thiolate tether.

2. Experimental section

2.1. General information

All reactions related to surface-modifications were carried out under Argon using standard Schlenk techniques and dry degassed solvents. TEOS was distilled from Mg. Et₃N was distilled from CaH₂. 1-hexene and 4-Phenyl-1-butene were distilled from Na, degassed and stored for 4 h over activated Selexsorb CD®. Dodecane was distilled from Na and degassed.

Elemental analyses were performed under inert atmosphere at the Mikroanalytisches Labor Pascher, Remagen, Germany. N analysis was based on the method of Dumas (instrument: N-analyser from Pascher). Ru, S, and Si analyses were performed by dissolution of the sample with acids and determination of the element concentration by ICP-AES (instrument: iCap 6500 from Thermo Fisher Scientific). Liquid ¹H NMR spectra were recorded on a Bruker AC 300 MHz. Proton chemical shifts are reported in ppm (δ) with the solvent reference relative to tetramethylsilane (TMS) employed as the internal standard (CDCl₃ δ = 7.26 ppm; CD₂Cl₂, δ = 5.32 ppm). Liquid ¹³C NMR spectra were recorded on a Bruker AC 300 MHz operating at 75 MHz, with complete proton decoupling. Carbon chemical shifts are reported in ppm (δ) relative to TMS with the respective solvent resonance as the internal standard (CDCl₃, δ = 77.16 ppm; CD₂Cl₂, δ = 54.00 ppm). CP-MAS NMR spectra were recorded on a Bruker Advance 300 MHz spectrometer with a conventional double resonance 4 mm CP-MAS probe. The MAS frequency was set to 10 kHz for all the ¹H and ¹³C experiments reported here. N₂ adsorption-desorption experiments were carried out on a Belsorb Japan system. DRIFT analyses were performed on a Nicolet 6700 FT-IR Spectrometer from Thermo Scientific. TEM micrographs were performed using a JEOL 2100 F electron microscope. The acceleration voltage was 200 kV. The samples were prepared by dispersing a drop of the ethanol suspension of a ground sample on a Cu grid covered by a carbon film.

2.2. Catalysis synthesis

2.2.1. Synthesis of S-(p-Methoxybenzyl)-4-ethynyl-2,6-diphenylthiophenol (5)

The synthesis of **5** was carried out as shown in Scheme 1 and as detailed below.

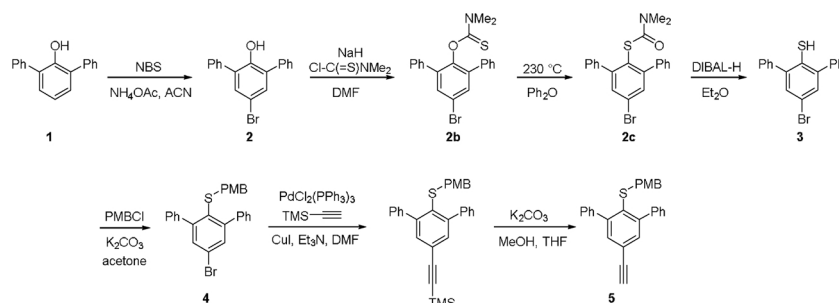
N-bromosuccinimide (7.5 g, 42 mmol) was added into a mixture of

2,6-diphenylphenol (**1**) (10 g, 40.6 mmol), NH₄OAc (616 mg, 20 mol%) and CH₃CN (200 mL) and stirred for 4 h at room temperature. Then, the solvent was removed under vacuum and the residual was taken with EtOAc (200 mL) and washed with H₂O (3 × 100 mL). The organic phases were dried with anhydrous Na₂SO₄, filtered and concentrated. The product (**2**) was purified by flash column chromatography (95:5, Petroleum ether/EtOAc). Yield: 11.5 g = 87 %.

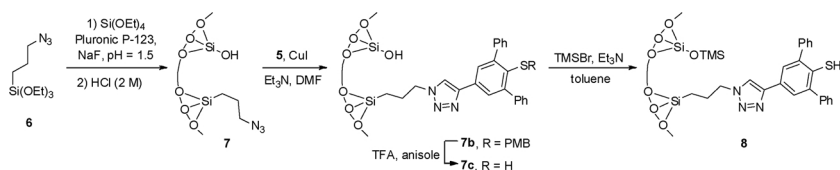
NaH (60 % mineral oil, 1.52 g, 38 mmol) and dry DMF (20 mL) were put into a three-neck flask equipped with a condenser and an addition funnel under Ar. Compound **2** (9.9 g, 30.4 mmol) was dissolved in dry DMF (30 mL) and added slowly via the addition funnel. Then, dimethylthiocarbamoyl chloride (4.5 g, 36.5 mmol) dissolved in dry DMF (20 mL) was added in the same way. The mixture was heated at 100 °C for 2 h. After cooling to room temperature, the solution was added into a 2 % w/w KOH aqueous solution (500 mL), the precipitate was filtered and washed with H₂O (3 × 300 mL). The product (**2b**) was purified by column chromatography (95:5, Petroleum ether/EtOAc). Yield: 10.0 g = 80 %. A mixture of compound **2b** (10.0 g, 24.3 mmol) and Ph₂O (30 mL) was heated to 245 °C under Ar for 72 h. Then, most of the Ph₂O was removed under vacuum and the concentrate was purified by flash column chromatography (85:15, Petroleum ether/EtOAc) to give product **2c**. Yield: 8.8 g = 88 %. Under Argon, DIBAL-H (1 M in THF, 45 mL, 45 mmol) was added dropwise onto a vigorously stirred mixture of compound **2c** (8.8 g, 21.3 mmol) and dry Et₂O (170 mL) at 0 °C. The reaction was stirred for 4 h at reflux temperature, whereupon more DIBAL-H (1 M in THF, 28 mL, 28 mmol) was added. The mixture was allowed to reflux overnight. Then, the reaction was cooled down to room temperature and added slowly into a mixture of crushed ice (500 mL) and concentrated H₂SO₄ (50 mL). The product was extracted with Et₂O (3 × 200 mL) and the combined organic phases were washed with an aqueous solution of potassium sodium tartrate (15 % w/w, 200 mL), dried with anhydrous Na₂SO₄, filtered and concentrated. The crude mixture was purified by flash column chromatography (99:1, Petroleum ether/EtOAc) to render product **3**. Yield: 5.4 g = 85 %.

p-Methoxybenzyl chloride (1050 μL, 7.6 mmol) was added to a solution of compound **3** (2.0 g, 5.9 mmol) and K₂CO₃ (1.6 g, 11.7 mmol) in acetone (60 mL) under Ar. The mixture was refluxed overnight. Then it was filtered, washed with DCM and the filtrate concentrated under vacuum. The product (**4**) was purified by flash column chromatography (99:1, Petroleum ether/EtOAc). Yield: 2.2 g = 81 %.

Compound **4** (600 mg, 1.3 mmol) was dissolved in dry DMF (11 mL) and dry Et₃N (11 mL) and Ar was bubbled in the solution for 1 h. Then, PdCl₂(PPh₃)₂ (136 mg, 15 mol%), CuI (74 mg, 30 mol%) and ethynyltrimethylsilane (572 μL, 4.1 mmol) were added. The mixture was stirred at 100 °C overnight. The solvent was removed under vacuum and the crude mixture was redissolved in EtOAc, filtered through a short pad of Celite and concentrated. The crude mixture was dissolved in dry MeOH (10 mL) and dry THF (10 mL), K₂CO₃ (1.0 g, 7.3 mmol) was added and the mixture was stirred at room temperature for 4 h. Then, the solvent was removed under vacuum and the crude redissolved in DCM, filtered and concentrated. The mixture was purified by flash column chromatography (98:2, Petroleum ether/EtOAc) to give S-(p-Methoxybenzyl)-4-ethynyl-2,6-diphenylthiophenol (**5**). Yield: 370 mg = 70 %.



Scheme 1. Synthesis of alkyne **5**. NBS: *N*-bromosuccinimide, ACN: acetonitrile, DMF: *N,N*-dimethylformamide, DIBAL-H: diisobutylaluminium hydride, PMBCL = 4-methoxybenzyl chloride, TMS: trimethoxysilyl, THF: tetrahydrofuran.



Scheme 2. Synthesis of the hybrid silica material. TFA: trifluoroacetic acid.

2.2.2. Synthesis of azidopropyl silica material **7**

The synthesis of **8** was carried out as shown in [Scheme 2](#) and as detailed below.

A homogeneous solution of P123 (8.4 g), H₂O (333 mL) and HCl 37 % (878 μ L) was added into a mixture of TEOS (20 mL, 90 mmol) and (azidopropyl)triethoxysilane (**6**) (560 mg, 2.25 mmol). The reaction mixture was stirred for 2 h at room temperature and then warmed up to 45 °C, at which NaF (154 mg, 3.67 mmol) was added when the solution reached 40 °C. The mixture was stirred at this 45 °C for 72 h. The resulting solid was filtered and washed with H₂O, EtOH, acetone and Et₂O. The surfactant was removed by Soxhlet extraction with EtOH during 48 h. The solid was then filtered, washed with acetone and Et₂O and dried at 135 °C under vacuum (10^{-2} mbar). The resulting material was suspended in HCl 2 M (500 mL) and stirred at 45 °C for 2 h. After filtration, washing with H₂O, EtOH, acetone and Et₂O and drying at 135 °C under vacuum (10^{-2} mbar) gave 4.2 g of material **7** were obtained as a white powder.

2.2.3. Immobilization of the ligand on the silica surface

Alkyne **5** (650 mg) and material **7** (1.78 g) were dispersed in dry DMF (30 mL) and dry Et₃N (3 mL), and the solution was degassed bubbling Ar for 30 min. Then, CuI (120 mg) was added and the mixture was stirred under Ar for 4 days at 50 °C. After this time, the solution was filtered and washed with acetone to recover the unreacted alkyne. The material from the filter was washed with an EDTA solution [5 g of EDTA + 40 mL of H₂O + 30 mL of DMF + 0.5 mL of Et₃N], H₂O, EtOH, acetone and Et₂O and then dried under vacuum (10^{-2} mbar) at 135 °C overnight. 2.1 g of material **7b** were obtained as a white powder. Material **7b** (2.1 g) was dispersed in trifluoroacetic acid (42 mL) and anisole (12.6 mL) and stirred for 72 h at room temperature. After this time, the solution was filtered and washed with H₂O, acetone and Et₂O and then dried under vacuum (10^{-2} mbar) at 135 °C overnight. The obtained material (1.9 g) was suspended in dry toluene (160 mL) and dry Et₃N (25 mL) under Ar, whereupon TMSBr (11.4 mL) was added. The mixture was stirred at room temperature for 72 h. The solid was filtered under Ar, washed with dry toluene, dry MeOH and dry Et₂O and then dried at 135 °C under vacuum (10^{-2} mbar). 2.1 g of material **8** were obtained as a white powder.

2.2.4. Immobilization of the catalyst via anion exchange

Material **8** (400 mg), dry toluene (4 mL) and potassium bis(trimethylsilyl)amide, KHMDS, (0.5 M solution in toluene, 1 mL) were stirred for 2 h at room temperature under Ar atmosphere. The solvent was filtered off and the material washed with more toluene (3×8 mL).

To the dry material, a solution of the Ru precursor (**HG-II**, **HG-II-NCO** or **M31**, 0.2 mmol) in toluene (8 mL) was added. The mixture was stirred for 20 h at room temperature. Subsequently, the solvent was filtered off and the material washed with dry DCM (3×10 mL). In the case of **C3**, the material was washed with DCM containing 1 % pyridine, to make sure that the pyridine ligand was not lost during washing. The material was dried under vacuum (10^{-2} mbar) for 20 h.

2.3. Experimental procedure for the catalytic tests

The immobilized catalyst (≈ 10 mg, ≈ 1 μ mol of Ru) was weighed in a 2 mL vial with a stirring magnet inside the glovebox. Then, the substrate (1 mmol) and the internal standard (dodecane) were added, the vial was capped, and the reaction was stirred at the desired temperature (20 or 40 °C) still inside the glovebox. Samples were collected at different times. Yields and Z-selectivity were analyzed by GC using the dodecane as reference.

3. Results and discussion

3.1. Synthesis and characterizations

Our approach was designed as follows: i) preparation of a bulky thiol, similar to the one present in **JO-1**, bearing a terminal alkyne moiety; ii) synthesis of a mesostructured silica material featuring a flexible azidopropyl group on the surface; iii) immobilization of the alkyne-thiol on the surface via a copper-catalyzed azide-alkyne cycloaddition (CuAAC); iv) immobilization of Ru olefin metathesis catalysts to the thiols via anion exchange [13].

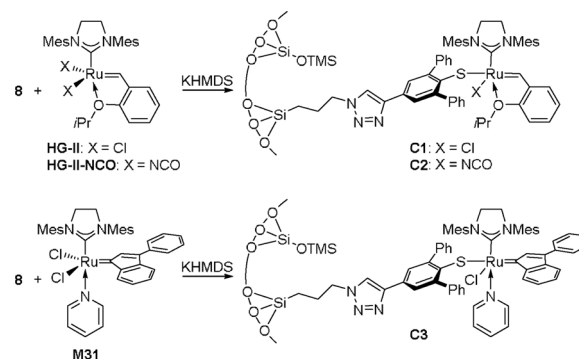
The synthesis of the bulky thiol bearing an alkyne moiety started by brominating the commercially available 2,6-diphenylphenol **1** to give bromophenol **2** ([Scheme 1](#)). Formation of the carbamate, followed by a Newman-Kwart rearrangement and cleavage of the thiocarbonate gave bromothiophenol **3**. The latter compound was protected as 4-methoxybenzyl thioether – stable enough to withstand the subsequent reactions and with a deprotection methodology suitable to be carried out when supported on the silica material.¹ Finally, a Sonogashira coupling

¹ Other protecting groups were tested without success. Protection as trimethylsilyl thioether was attempted in different conditions, but no silylation product was ever observed probably due to the steric hindrance of the two ortho-phenyl substituents. The protection as tert-butyl thiocarbonate proceeded well, but it was partially deprotected during the subsequent Sonogashira

with ethynyltrimethylsilane and subsequent desilylation yielded compound **5**, bearing a terminal alkyne and a protected thiol.

In parallel, a mesostructured hybrid silica material containing azidopropyl surface fragments was prepared by a sol-gel process using a templating route (Scheme 2) [14]. This was achieved by co-hydrolysis and co-condensation of one equivalent of (azidopropyl)triethoxysilane and 40 equivalents of tetraethoxysilane in the presence of Pluronic® P-123 as the structure-directing agent. A subsequent acidic treatment was used to hydrolyze the remaining ethoxy groups on the silica surface. This methodology allows for an accurate control of the loading and a homogeneous distribution of the azidopropyl units inside the silica pore channels [14]. At this point, alkyne **5** was anchored to the surface via a CuAAC. The reaction was monitored by the appearance of signals in the aromatic region of the ^{13}C CP-MAS NMR spectrum and by the decrease of the $\nu(\text{N}=\text{N})$ band from the azido-group in the DRIFT spectrum (Figures S12 and S16). Elemental analysis indicated that 66 % of the azido groups reacted to give the cycloaddition product. The deprotection of the thiol involved a treatment with neat trifluoroacetic acid in the presence of anisole. A quantitative deprotection was accomplished as observed by the complete disappearance of the 4-methoxybenzyl peaks by NMR (Figure S12). Finally, the silica surface was passivated by treating the material with bromotrimethylsilane in the presence of triethylamine as the base.² In this way, we were able to produce material **8** at the gram-scale without affecting the structure of the silica material, as shown by N_2 adsorption-desorption isotherms and TEM microscopy (Figures S1 and S17).

As the last step, the catalyst was immobilized on the silica surface via an anionic exchange of one chloride by the thiolate tether. We had already observed that KHMDS was incompatible with Ru olefin metathesis catalysts [12], thus material **8** was first deprotonated with the base and all the excess removed by washings with toluene. The thiolate-containing material was then stirred with the corresponding Ru precursor in toluene to afford catalysts **C1**, **C2**, and **C3** (Scheme 3). The color of the final supported complexes was a lighter version of their homogeneous precursors: green for **C1** and **C2** and orange-brownish for **C3**. ^{13}C CP-MAS NMR showed the expected signals after the immobilization of the Ru complexes (Figures S13, S14 and S15): aromatic peaks ($\delta = 120\text{--}140$ ppm) from the mesitylene and alkylidene moieties, a peak at $\delta \approx 50$ ppm corresponding to aliphatic carbons attached to a nitrogen, and the rest of aliphatic peaks at $\delta = 10\text{--}20$ ppm. As expected from the fact that ^{13}C labels were not used, the carbenic signal was not observed. The difficulty in observing such carbenic signals, even using cutting edge NMR methods such as Dynamic Nuclear Polarization, is due to the inherent large CSA [15] for this type of complexes and the absence of protons in the vicinity of the carbenic carbon. The S/Ru ratios found by elemental analysis correspond to 45 % grafting of thiolate groups for **C1**, 58 % for **C2** and 72 % for **C3**.³ As we had already observed with other thiolate linkers [12], the grafting yields are much higher than those obtained when grafting Ru olefin metathesis catalysts through the NHC moiety [11].



Scheme 3. Immobilization of different homogeneous catalysts on material **8** to give catalysts **C1**, **C2** and **C3**.

3.2. Catalytic tests

Next, we turned to the exploration of the metathesis activity and selectivity of these complexes (Table 1). The turnover number (TON) towards the desired product and the Z-selectivity of each catalyst was investigated in different conditions under inert atmosphere. The homometathesis of 1-hexene (**S1**) with catalyst **C1** at room temperature achieved a TON of 98 and a moderate Z-selectivity of 63 % after 7 h of reaction (entry 3). These results are comparable to those of its homogeneous counterpart **JO-1** after the same reaction time (TON = 99 and 68 % of Z-isomer, entry 2). Both catalysts are still far from the activities of the non-Z-selective **HG-II** standard (TON = 583 at 7 h, entry 1). Interestingly, while **JO-1** shows the higher Z-selectivities at short reaction times (81 % of Z after 1 h), **C1** displays a profile with a maximum of Z-selectivity after a few hours (see Fig. 3). This finding might seem counterintuitive, since the reversibility of the metathesis reaction should drag the product selectivity to the thermodynamic equilibrium (16 % of Z-5-decene). Thus, the Z-selectivity should in theory decrease with time, as observed with **JO-1** (Table 1, entry 2). A plausible explanation for the observed behavior might be that this supported catalyst, which is very sterically hindered due to its ligands and to the presence of the silica surface, may require a longer induction period to get activated and to reach its most Z-selective conformation. Then, after reaching a maximum, the ratio of Z-isomer starts decreasing, as expected. Another observation from the kinetic profile (Fig. 3) is that the catalyst loses almost all activity after 7–8 h. An increase of the temperature to 40 °C (Table 1, entry 4) accelerated the reaction, but did not affect the Z-selectivity or the catalyst TON. Unfortunately, these catalysts (both the homogeneous and the supported one) decompose very fast, leading to isomerization catalysts (probably Ru hydrides) which lost all the metathesis activity, thus preventing their recyclability. However, this findings proof that the main deactivation pathway of the catalyst doesn't follow a bimolecular process, as it is often observed in metal catalysis [16], but an intramolecular process as the rigidity of the silica and the homogeneous distribution of the catalysts along the surface hamper the possibility of two metallic centers getting in close proximity.

In order to prevent the formation of Ru hydride species that lead to higher isomerization degrees, different additives commonly used to this aim [17] were tested. DMAN (1,8-bis(dimethylamino)naphthalene), a strong and bulky base used to trap any proton in solution, produced the opposite effect, slightly increasing the amount of isomerization but without affecting the metathesis activity (entries 5 and 6). Tricyclohexylphosphine oxide reduced the amount of isomerization products and increased the Z-selectivity up 78 %, however, at expenses of the activity (entry 7). The use of 1,4-benzoquinone as additive completely suppressed isomerization but also the metathesis activity (TON = 9 after 7 h, entry 8). Solvents, such as DCM or THF (entries 9 and 10), greatly reduced the catalyst activity. However, THF enhanced the Z-

(footnote continued)

coupling. A most robust protection as n-butyl thioether was perfectly suitable for the preparation of the material, however, no conditions were found for its deprotection once supported.

² The thiol group was not silylated during the passivation of the surface. Attempts to prepare the trimethylsilyl thioether in homogeneous conditions were unsuccessful, probably due to the steric hindrance of the two ortho-phenyl substituents.

³ Due to the lower stability of M31 compared to HG-II, degradation of the catalysts probably occurred during the immobilization giving a Ru/S ratio of 1.1. The correct yield of immobilization was calculated from the N/S ratio (see Supporting Information).

Table 1
Catalytic results on the homometathesis of 1-hexene (**S1**) and 4-phenyl-1-butene (**S2**).

<chem>CCCCC=C</chem> 1-hexene (S1) $\xrightarrow[\text{Neat}]{\text{C1-3 (0.1 mol\%)}}$ <chem>CCCCC=CCCC</chem> 5-decene (P1)								
#	catalyst	additive	T (°C)	t (h)	side products (%) ^{[a],[b]}	yield P1 (%) ^[b]	TON to P1	% Z-selectivity ^{[b],[c]}
1	HG-II	–	20	7	4.9	58.3	583	16
2	JO-1	–	20	1	0.8	2.3	23	81
				7	6.9	9.9	99	68
3	C1	–	20	1	6.3	3.9	39	49
				7	20.0	9.8	98	63
4	C1	–	40	3	27.5	10.1	101	63
5	C1	DMAN (2 eq./cat)	20	7	45.0	10.7	107	63
6	C1	DMAN (20 eq./cat)	20	7	46.0	9.6	96	65
7	C1	OPCy ₃ (5 eq./cat)	20	7	6.6	5.5	55	78
8	C1	p-BQ (5 eq./cat)	20	7	0.0	0.9	9	50
9	C1	DCM (200 µl)	20	7	26.1	0.8	8	41
10	C1	THF (200 µl)	20	7	54.0	1.5	15	70
11	C2	–	20	7	20.9	5.5	55	55
12	C2	–	40	3	21.1	4.7	47	60
13	C2	in air	20	7	0.4	0.5	5	81
14	C3	–	20	1	3.8	1.4	14	76
				7	16.9	1.8	18	71
15	C3	pyridine (50 eq./cat)	20	7	0	0	0	–
<chem>Ph-CH=CH-CH2-CH3</chem> 4-phenyl-1-butene (S2) $\xrightarrow[\text{Neat}]{\text{C1-3 (0.1 mol\%)}}$ <chem>Ph-CH=CH-CH2-CH2-Ph</chem> 1,6-diphenyl-3-hexene (P2)								
#	catalyst	additive	T (°C)	t (h)	side products (%) ^{[d],[b]}	yield P2 (%) ^[b]	TON to P2	% Z-selectivity ^{[b],[c]}
16	HG-II	–	40	7	23.6	25.7	257	21
17	JO-1	–	40	0.2	7.8	4.1	41	84
				0.6	18.1	9.6	96	78
18	C1	–	40	7	76.0	9.9	99	74
19	C2	–	40	7	54.5	5.1	51	71
20	C2	in air	40	7	0.9	1.4	14	81
21	C3	–	40	7	25.4	1.8	18	77

[a] includes *n*-pentene, *n*-hexene and *n*-heptene isomers (except **S1**) and 4-nonene. [b] calculated from GC analysis using dodecane as internal standard. [c] % of Z-isomer in the product (**P1** or **P2**) [d] includes phenylpropene, phenylbutene and phenylpentene isomers (except **S2**) and 1,5-diphenyl-2-pentene and 1,4-diphenyl-2-butene. DMAN = 1,8-Bis(dimethylamino)naphthalene. p-BQ = *para*-benzoquinone.

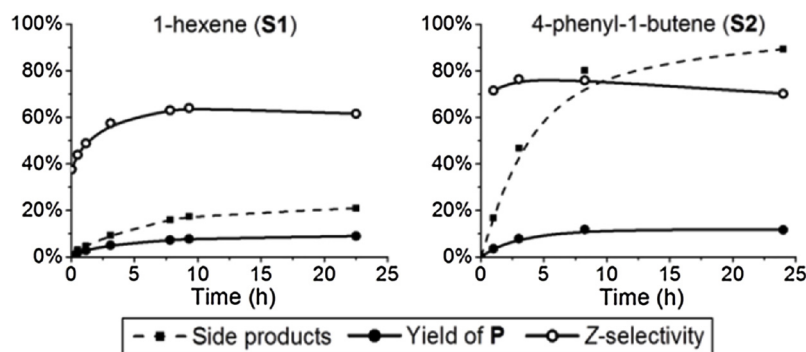


Fig. 3. Evolution of the metathesis reactions of Table 1, entry 3 and entry 18 vs time.

selectivity to 70 %.

Catalyst **C2**, equivalent to **C1** but bearing an isocyanate instead of chloride, displayed lower activities and slightly lower Z-selectivities (Table 1, entry 11 vs 3). Jensen and co-workers had reported that its homogeneous analogue **JO-2** performed better when used in air – with increased Z-selectivity and less isomerization at the expense of catalytic activity [7b]. Indeed, when testing **C2** in air (entry 13), we observed a remarkable increase in Z-selectivity (reaching 81 %) and less isomerization products. However, the activity dropped significantly. In the case of **C3**, bearing an indenylidene moiety and a coordinated pyridine, a fast decomposition of the catalyst (little activity after 1 h) but high Z-selectivities (up to 76 %) were observed (entry 14). These selectivities are comparable to those obtained with **C1** in THF (entry 10). In both cases the presence of a coordinating molecule (THF or pyridine) might

favor a particular conformation of the thiolate ligand which is much more Z-selective. We therefore added an excess of pyridine to the reaction (entry 15), but in that case no activity was detected after 7 h. This might be explained by the fact that the coordinatively saturated Ru complex is overstabilized by the excess of pyridine or due to a pyridine-triggered catalyst decomposition via a nucleophilic attack on the alkylidene.

The use of 4-phenyl-1-butene (**S2**) as substrate resulted in similar activities, but with more isomerization. However, due to the increased bulkiness of the substrate, the Z-selectivities were also superior, showing again a maximum at around 7 h (Fig. 3). The selectivity of **C1** was again similar to that of its homogeneous counterpart **JO-1**. The TONs were also comparable (Table 1, entry 17 vs 18), but the reaction mediated by **C1** was slower and the catalyst lost its metathesis activity

after 7–8 h. As with 1-hexene, **C2** exhibited lower activities and enhanced Z-selectivity when used in air (entries 19 and 20). The Z-selectivity of **C3** in metathesis of **S2** was good (77 %) but the activity was very low (TON = 18 after 7 h).

4. Conclusions

To conclude, we have successfully developed a series of heterogenized Z-selective 2,4,6-triphenylbenzenethiolate-Ru olefin metathesis catalysts. To reach this goal, a mesostructured hybrid silica material containing a sterically demanding aryl thiol on the surface has been prepared and the complex was generated *in situ* by an anionic exchange. The activity of these new catalysts was found comparable to those of their homogeneous counterparts, with TONs on up to 107 at Z-selectivities of 63 %, with the advantage that the supported catalyst can be easily removed. Z-selectivities of up to 81 % could be achieved at very low TON (TON = 5). The similar activities between the homogeneous and heterogeneous counterparts suggest that the deactivation pathway for this type of Ru complexes is more likely intramolecular and not intermolecular. Remarkably, the fact that no activity/selectivity is lost during immobilization is promising for the immobilization of related more active Z-selective or stereoretentive thiolate-coordinated ruthenium-based olefin metathesis catalysts.

Author contribution

Dr. Renom-Carrasco: Designed and performed experiments, prepared the materials and performed catalytic tests, wrote the paper

Dr. Philipp Mania: Performed research on ligand development

Dr. Reine Sayah: Designed and performed experiments concerning the ligands

M. Laurent Veyre: Ran analyses and performed characterization of materials (TEM, Adsorption experiments)

Dr. Giovanni Occhipinti: Designed and performed experiments concerning the preparation of molecular complexes and catalytic tests

Prof. Vidar R. Jensen: Supervised and designed research on the molecular complexes, wrote the paper

Dr. C. Thieuleux: Supervised and designed research on the catalytic materials, wrote the paper

Declaration of Competing Interest

The authors declare that they have no known competing financial interests or personal relationships that could have appeared to influence the work reported in this paper.

Acknowledgements

The authors gratefully acknowledge financial support from the Research Council of Norway via the GASSMAKS program (grant number 208335) and the FRIPRO program (262370). The authors would also like to acknowledge Prof. Christophe Copéret for fruitful discussions.

Appendix A. Supplementary data

Supplementary material related to this article can be found, in the online version, at doi:<https://doi.org/10.1016/j.mcat.2019.110743>.

References

- [1] R.H. Grubbs, *Handbook of Metathesis* Vol. 1 Wiley-VCH, Weinheim, 2003.
- [2] (a) M.M. Flook, A.J. Jiang, R.R. Schrock, P. Müller, A.H. Hoveyda, Z-selective olefin metathesis processes catalyzed by a molybdenum hexaisopropylterphenoxide monopyrrolide complex, *J. Am. Chem. Soc.* 131 (2009) 7962–7963; (b) I. Ibrahim, M. Yu, R.R. Schrock, A.H. Hoveyda, Highly z- and enantioselective ring-opening/cross-metathesis reactions catalyzed by Stereogenic-at-Mo adamantlylimido complexes, *J. Am. Chem. Soc.* 131 (2009) 3844–3845;
- (c) A.J. Jiang, Y. Zhao, R.R. Schrock, A.H. Hoveyda, Highly Z-Selective metathesis homocoupling of terminal olefins, *J. Am. Chem. Soc.* 131 (2009) 16630–16631.
- [3] (a) S.C. Marinescu, R.R. Schrock, P. Müller, M.K. Takase, A.H. Hoveyda, Room-temperature Z-Selective homocoupling of α -Olefins by tungsten catalysts, *Organometallics* 30 (2011) 1780–1782; (b) E.M. Townsend, J. Hyvl, W.P. Forrest, R.R. Schrock, P. Müller, A.H. Hoveyda, Synthesis of molybdenum and tungsten alkylidene complexes that contain sterically demanding arenethiolate ligands, *Organometallics* 33 (2014) 5334–5341; (c) J.K. Lam, C. Zhu, K.V. Bukhryakov, P. Müller, A.H. Hoveyda, R.R. Schrock, Synthesis and evaluation of molybdenum and tungsten monoaryloxide halide alkylidene complexes for Z-Selective cross-metathesis of cyclooctene and Z-1,2-Dichloroethylene, *J. Am. Chem. Soc.* 138 (2016) 15774–15783; (d) E.C. Yu, B.M. Johnson, E.M. Townsend, R.R. Schrock, A.H. Hoveyda, Synthesis of linear (Z)- α,β -Unsaturated esters by catalytic cross-metathesis. The influence of acetonitrile, *Angew. Chem. Int. Ed.* 55 (2016) 13210–13214; (e) M. Joo Koh, T.T. Nguyen, J.K. Lam, S. Torker, J. Hyvl, R.R. Schrock, A.H. Hoveyda, Molybdenum chloride catalysts for Z-selective olefin metathesis reactions, *Nature* 542 (2017) 80–85.
- [4] X. Shen, T.T. Nguyen, M.J. Koh, D. Xu, A.W.H. Speed, R.R. Schrock, A.H. Hoveyda, Kinetically E-selective macrocyclic ring-closing metathesis, *Nature* 541 (2017) 380–385.
- [5] (a) K. Endo, R.H. Grubbs, Chelated ruthenium catalysts for Z-Selective olefin metathesis, *J. Am. Chem. Soc.* 133 (2011) 8525–8527; (b) B.K. Keitz, K. Endo, M.B. Herbert, R.H. Grubbs, Z-selective homodimerization of terminal olefins with a ruthenium metathesis catalyst, *J. Am. Chem. Soc.* 133 (2011) 9686–9688.
- [6] M.B. Herbert, R.H. Grubbs, Z-Selective cross metathesis with ruthenium catalysts: synthetic applications and mechanistic implications, *Angew. Chem. Int. Ed.* 54 (2015) 5018–5024.
- [7] (a) G. Occhipinti, F.R. Hansen, K.W. Törnroos, V.R. Jensen, Simple and highly Z-Selective ruthenium-based olefin metathesis catalyst, *J. Am. Chem. Soc.* 135 (2013) 3331–3334; (b) G. Occhipinti, V. Koudriavtsev, K.W. Törnroos, V.R. Jensen, Theory-assisted development of a robust and Z-selective olefin metathesis catalyst, *Dalton Trans.* 43 (2014) 11106–11117; (c) W. Smit, V. Koudriavtsev, G. Occhipinti, K.W. Törnroos, V.R. Jensen, Phosphine-based Z-Selective ruthenium olefin metathesis catalysts, *Organometallics* 35 (2016) 1825–1837; (d) G. Occhipinti, K.W. Törnroos, V.R. Jensen, Pyridine-stabilized fast-initiating ruthenium monothiolate catalysts for Z-Selective olefin metathesis, *Organometallics* 36 (2017) 3284–3292; (e) V.R. Jensen, G. Occhipinti, Pyridine-stabilized fast-initiating ruthenium monothiolate catalysts for Z-Selective olefin metathesis, *Int. Patent Appl.* (2017) WO 201709232.
- [8] (a) R.K.M. Khan, S. Torker, A.H. Hoveyda, Readily accessible and easily modifiable Ru-Based catalysts for efficient and Z-Selective ring-opening metathesis polymerization and ring-opening/cross-metathesis, *J. Am. Chem. Soc.* 135 (2013) 10258–10261; (b) M. Joo Koh, R.K.M. Khan, S. Torker, M. Yu, M.S. Mikus, A.H. Hoveyda, High-value alcohols and higher-oxidation-state compounds by catalytic Z-selective cross-metathesis, *Nature* 517 (2015) 181–186; (c) T.S. Ahmed, R.H. Grubbs, Fast-initiating, ruthenium-based catalysts for improved activity in highly E-Selective cross metathesis, *J. Am. Chem. Soc.* 139 (2017) 1532–1537.
- [9] C. Copéret, A. Comas-Vives, M.P. Conley, D.P. Estes, A. Fedorov, V. Mougél, H. Nagae, F. Núñez-Zarur, P.A. Zhizhko, Surface organometallic and coordination chemistry toward single-site heterogeneous catalysts: strategies, methods, structures, and activities, *Chem. Rev.* 116 (2016) 323–421.
- [10] (a) M.R. Buchmeiser, K. Grela (Ed.), *Olefin Metathesis - Theory and Praxis*, J. Wiley & Sons, 2014, pp. 495–514; (b) L. Xia, T. Peng, G. Wang, X. Wen, S. Zhang, L. Wang, Grubbs catalysts immobilized on Merrifield resin for metathesis of leaf alcohols by using a convenient recycling approach, *ChemistryOpen*, (2019), pp. 45–48; (c) H. Balcar, J. Čejka, Mesoporous molecular sieves as advanced supports for olefin metathesis catalysts, *Coord. Chem. Rev.* (2013), pp. 3107–3124.
- [11] (a) I. Karame, M. Boualleg, J.M. Camus, T.K. Maishal, J. Alauzun, J.M. Basset, C. Copéret, R.J.P. Corriu, E. Jeanneau, A. Mehdi, C. Réyé, L. Veyre, C. Thieuleux, Tailored Ru-NHC heterogeneous catalysts for alkene metathesis, *Chem. Eur. J.* 15 (2009) 11820–11823; (b) M.K. Samantary, J. Alauzun, D. Gajan, S. Kavitate, A. Mehdi, L. Veyre, M. Lelli, A. Lesage, L. Emsley, C. Copéret, C. Thieuleux, Evidence for metal–surface interactions and their role in stabilizing well-defined immobilized Ru–NHC alkene metathesis catalysts, *J. Am. Chem. Soc.* 135 (2013) 3193–3199.
- [12] M. Renom-Carrasco, P. Mania, R. Sayah, L. Veyre, G. Occhipinti, D. Gajan, A. Lesage, V.R. Jensen, C. Thieuleux, Supported Ru olefin metathesis catalysts via a thiolate tether, *Dalton Trans.* 48 (2019) 2886–2890.
- [13] C. Copéret, M. Chabanas, R. Petroff Saint-Arroman, J.-M. Basset, Homogeneous and heterogeneous catalysis: bridging the gap through surface organometallic chemistry, *Angew. Chem. Int. Ed.* 42 (2003) 156–181.
- [14] (a) S.L. Burkett, S.D. Sims, S. Mann, Synthesis of hybrid inorganic–organic mesoporous silica by co-condensation of siloxane and organosiloxane precursors, *Chem. Commun.* (1996) 1367–1368; (b) D.J. Macquarrie, Direct preparation of organically modified MCM-type materials. Preparation and characterisation of aminopropyl–MCM and 2-cyanoethyl–MCM, *Chem. Commun.* (1996) 1961–1962; (c) D. Margolese, J.A. Melero, S.C. Christiansen, B.F. Chmelka, G.D. Stucky, Direct

syntheses of ordered SBA-15 mesoporous silica containing sulfonic acid groups, *Chem. Mater.* 12 (2000) 2448–2459;

(d) L. Mercier, T.J. Pinnavaia, Direct synthesis of hybrid organic–Inorganic nanoporous silica by a neutral amine assembly route: structure–Function control by stoichiometric incorporation of organosiloxane molecules, *Chem. Mater.* 12 (2000) 188–196;

(e) For a review, see: F. Hoffmann, M. Cornelius, J. Morell, M. Fröba, Silica-based mesoporous organic–inorganic hybrid materials, *Angew. Chem. Int. Ed.* 45 (2006) 3216–3251 and 37.M. P. Conley, C. Copéret, C. Thieuleux C. Mesostructured Hybrid

Organic-Silica Materials: Ideal Supports for Well-Defined Heterogeneous Organometallic Catalysts *ACS Catalysis* 4 (2014) 1458–1469.

- [15] K. Yamamoto, C.P. Gordon, W.-C. Liao, C. Copéret, C. Raynaud, O. Eisenstein, Orbital analysis of Carbon-13 chemical shift tensors reveals patterns to distinguish Fischer and schrock carbenes, *Angew. Chem. Int. Ed.* 56 (2017) 10127–10131.
- [16] R.H. Crabtree, Deactivation in homogeneous transition metal catalysis: causes, avoidance, and cure, *Chem. Rev.* 115 (2015) 127–150.
- [17] S.H. Hong, D.P. Sanders, C.W. Lee, R.H. Grubbs, Prevention of undesirable isomerization during olefin metathesis, *J. Am. Chem. Soc.* 127 (2005) 17160–17161.